Neutron Binding Energies from (d, p) Reactions and Nuclear Shell Structure*

J. A. HARVEY
Laboratory for Nuclear Science and Engineering, Massachusetts Institute of Technology, Cambridge, Massachusetts
(Received September 21, 1950)

Using 14-Mev deuterons from the M.I.T. cyclotron, proton spectra have been measured for many heavy and medium atomic weight elements. The range of the protons was measured in aluminum foils by the method of "peaking" with a triple proportional counter. From the Q-value of the ground-state proton group (measured relative to a Q-value of 5.50 Mev for the aluminum ground-state group), the neutron binding energy of the residual nucleus has been obtained. These values are compared to the maximum gamma-ray energy obtained from thermal neutron capture. A few neutron binding energies have been measured from the (d, t) reaction and are compared with values obtained from the (γ, n) threshold. Several neutron binding energies have been computed from radioactive decay energies and measured neutron binding energies. All neutron binding energies have been compared with the values predicted from the semi-empirical mass formula. A sharp drop in neutron binding energy of about 2.2 Mev occurs at the completion of the closed shell of 126 neutrons. A drop, a little greater than 2 Mev, occurs at 50 neutrons. There is also a decrease in the region of 82 neutrons. There also seems to be a decrease of about 1 Mev in the region of 29 neutrons, but this is not very conclusive.

The differential cross section of the ground-state peaks from even Z, odd A isotopes at forward angles are much smaller (about a factor of ten) than the differential cross sections of the ground-state peaks from the same Z but even A isotopes. The ground-state peaks from Sn^{117} and Pb^{207}, however, are about 50 percent that of the even A isotopes.

I. INTRODUCTION

TO explain observed properties of nuclei, two models have been used, (a) the independent particle concept, and (b) the strong interaction viewpoint. Although the strong interaction picture successfully accounts for many nuclear phenomena, the single-particle model has received much attention by many writers.[1–7] Recently, many nuclear properties such as the natural abundances of the stable isotopes,[1] spins,[2] magnetic moments,[2] radioactive transitions,[2] isomerism,[2] quadrupole moments,[3] neutron capture cross sections,[4] and nuclear fission[5] have been analyzed in the light of a shell model and the existence of "magic numbers" has been definitely established.

It has also been pointed out[1, 8–16] that when a shell is completed, we should expect a nucleus of particular stability. When a new shell is begun, the binding energy of newly added particles will be less than that of the particles which completed the shell. This was shown[8] to be true for O^{16}. Considering only the masses of $A=4n$ nuclei, Smart[9] concluded that closed shells occur at mass numbers of 20 and 32. From a careful study of decay energies of the natural radioactive series and the semi-empirical mass formula, the binding energy of the last neutron and of the last proton has been predicted in the lead region.[10–15] Upon completion of the closed shell of 126 neutrons there is a decrease in neutron binding of about 2 Mev, and a decrease in proton binding energy of the order of 2.5 Mev after completing a closed shell of 82 protons. From a consideration of the nuclear stability in the region of 82 neutrons, Mayer[1] has suggested a drop in neutron binding energy of the order of 2 Mev after filling up the shell of 82 neutrons. Also Hanson *et al.*[17] have explained the high values of the (γ, n) thresholds in Zr^{90} and Mo^{92} as due to the particular stability of 50 neutrons. Recently,[18] precise mass measurements have indicated a sudden break in the packing fraction curve in the neighborhood of Zr^{90}, and possibly in the region of 28 neutrons. Masses in the region of calcium do not show any shell effect[19] with the exception of Ca^{40}.

II. METHODS OF MEASURING NEUTRON BINDING ENERGIES

The binding energy of the last neutron can be measured in many ways which can be conveniently divided into two groups. The first group includes the measurement of the energy required to remove a neutron from a stable nucleus represented by the threshold of the

* Part of a thesis submitted in partial fulfillment of the requirements for the degree of Doctor of Philosophy in Physics in the Graduate School of the Massachusetts Institute of Technology. This work was supported by the joint program of the ONR and the AEC. Some of these results were reported at the New York Meeting (February, 1950) and the Washington Meeting (April, 1950) of the American Physical Society.

[1] Maria G. Mayer, Phys. Rev. **74**, 235 (1948); W. D. Harkins and M. Popelka, Jr., Phys. Rev. **76**, 989 (1949).
[2] E. Feenberg, Phys. Rev. **75**, 320 (1949); E. Feenberg and K. C. Hammack, Phys. Rev. **75**, 1877 (1949); L. W. Nordheim, Phys. Rev. **75**, 1894 (1949); Feenberg, Hammack, and Nordheim, Phys. Rev. **75**, 1968 (1949).
[3] W. Gordy, Phys. Rev. **76**, 139 (1949); R. D. Hill, Phys. Rev. **76**, 998 (1949); Townes, Foley, and Low, Phys. Rev. **76**, 1415 (1949); J. Rainwater, Phys. Rev. **79**, 432 (1950).
[4] D. J. Hughes and D. F. Sherman, Phys. Rev. **78**, 632 (1950).
[5] D. C. Brunton, Phys. Rev. **76**, 1798 (1949); L. E. Glendenin, Phys. Rev. **77**, 755 (1950).
[6] Maria G. Mayer, Phys. Rev. **75**, 1969 (1949); Haxel, Jensen, and Suess, Phys. Rev. **75**, 1766 (1949).
[7] E. Feenberg, Phys. Rev. **76**, 1275 (1949); E. Feenberg, Phys. Rev. **77**, 771 (1950); Maria G. Mayer, Phys. Rev. **78**, 16, 22 (1950).
[8] H. A. Bethe and R. F. Bacher, Revs. Modern Phys. **8**, 171 (1936).
[9] J. S. Smart, Phys. Rev. **76**, 439 (1949).
[10] W. Elsasser, J. phys. radium **5**, 635 (1934).
[11] A. Berthelot, J. phys. radium (VIII) **3**, 17 (1942).
[12] S. von Flügge and J. Mattauch, Physik. Z. **44**, 181 (1943).
[13] M. Stern, Revs. Modern Phys. **21**, 316 (1949).
[14] K. Way, Phys. Rev. **75**, 1448 (1949).
[15] A. H. Wapstra, Physica **16**, 33 (1950).
[16] Perlman, Ghiorso, and Seaborg, Phys. Rev. **77**, 27 (1950).
[17] Hanson, Duffield, Knight, Diven, and Palevsky, Phys. Rev. **76**, 578 (1949).
[18] Duckworth, Woodcock, and Preston, Phys. Rev. **79**, 198 (1950).
[19] C. H. Townes and W. Low, Phys. Rev. **79**, 198 (1950).

(γ, n)[17,20–26] or the $(n, 2n)$ reaction,[27] the Q-value of the ground-state group from a (p, d) reaction[28] or a (d, t) reaction.[29] Nearly 40 neutron binding energies have been obtained from photo-neutron thresholds. The reported values are measured relative to the Cu^{63} threshold at 10.9 Mev and are accurate to 100 or 200 kev. The only $(n, 2n)$ threshold reported is that of Cu^{63}, giving a value of 11.2 ± 0.3 Mev in good agreement with the photo-neutron threshold. The (p, d) reaction has been observed with low energy protons on beryllium and with high energy protons on carbon.[28] The Q-value for a (d, t) reaction is only slightly negative, since the binding energy of the last neutron in a triton is over 6 Mev. Triton groups have been observed in several heavy elements and the neutron binding energy derived from the Q-value of the highest energy group agrees with (γ, n) threshold measurements. If the residual nucleus is not left in its ground state, then only an upper limit to the neutron binding energy is obtained by these methods.

The second group consists in the measurement of the energy released on the addition of a neutron to a stable nucleus by the gamma-rays from thermal neutron capture or the Q-value of the ground-state proton group from a (d, p) reaction. A search for high energy gamma-rays has been made by Kubitschek and Dancoff,[30] using an absorption method, and by Kinsey *et al.*,[31–33] using a pair spectrometer. The resolution obtained with the spectrometer is about 100 kev and gamma-ray energies can be measured to an accuracy of 10–20 kev. For targets containing more than one isotope the highest energy gamma-ray is assigned to the lowest odd A isotope in the target. Results obtained by this method will be compared to the results obtained from the (d, p) method. Since a (d, p) reaction is simply the transfer of a neutron from the deuteron to the target nucleus, the Q-value for the reaction is equal to the difference between the neutron binding energy in the residual nucleus and the deuteron binding energy. Prior to the present research very little work[34–38] had been done with nuclei heavier than calcium and then only up to arsenic ($A=75$). Both of these methods measure the neutron binding energy in the residual nucleus, which has one more neutron than the target nucleus. Also, if the residual nucleus is not left in the ground state then only a lower limit for the neutron binding energy is obtained. The (d, p) method has the advantage, in principle at least, that coincidences between protons and gamma-rays can be searched for, and if no coincidences are found, then it can be concluded that the proton group observed truly leaves the nucleus in its ground state. However, the counting rates are very low and the work done to date is not conclusive.

If the neutron binding energy measured by the (d, p) or (n, γ) method agrees with the value obtained by the (γ, n) or (d, t) method, then we know that this value is the true value. Using decay energies of neighboring isobars we can also check several other values measured by the (d, p) and (γ, n) methods. A few cycles can be completed to check several values as a group; for example, the cycle involving the alpha-decay energy of Po^{210} or the mass difference of Fe^{54} and Fe^{56} from mass spectrographic measurements.[39]

In a few cases, neutron energies can be computed from decay energies and a measured neutron binding energy. However, it is necessary that the total decay energy be known or else one obtains only an upper or a lower limit. This method is very useful in the lead region where the total decay energies of nearly all the elements are well known.

III. DESCRIPTION OF APPARATUS

The equipment is the same as that described by Boyer, *et al.*,[40] and only the details pertinent to the accurate measurement of Q-values shall be given here. The 15.5-Mev deuteron beam from the cyclotron is "piped" from the cyclotron and focused at the center of the target chamber about 12 feet from the cyclotron. Targets are mounted in small aluminum frames 1 inch square at the center of the target chamber. The targets can be retracted into the target holder and inserted into the deuteron beam by compressed air. A target can also be inserted into the deuteron beam through a side port and alternate runs can be taken on the two targets and one target can be used for a reference. The targets used were about 20 mg/cm^2 thick. The deuteron beam was uniformly spread over $\frac{1}{2}$ inch square on the target. The protons were detected by a triple proportional counter and their range measured in aluminum absorbers by the principle of "peaking," so that only protons ending their range in the third counter were counted. The triple counter and absorbers can be rotated in angle, and thus the proton spectrum can be

[20] G. C. Baldwin and H. W. Koch, Phys. Rev. **67**, 1 (1945).
[21] McElhinney, Hanson, Becker, Duffield, and Diven, Phys. Rev. **75**, 542 (1949).
[22] H. Palevsky and A. O. Hanson, Phys. Rev. **79**, 242 (1950).
[23] W. E. Ogle and R. E. England, Phys. Rev. **78**, 63 (1950.)
[24] Ogle, Brown, and Carson, Phys. Rev. **78**, 63 (1950).
[25] R. W. Parsons and C. H. Collie, Proc. Phys. Soc. London **A63**, 839 (1950).
[26] R. W. Parsons, *et al.*, Proc. Phys. Soc. London **A63**, 915 (1950).
[27] J. L. Fowler and J. M. Slye, Jr., Phys. Rev. **77**, 787 (1950).
[28] Levinthal, Martinelli, and Silverman, Phys. Rev. **78**, 199 (1950).
[29] J. A. Harvey, Phys. Rev. **79**, 241 (1950).
[30] H. E. Kubitschek and S. M. Dancoff, Phys. Rev. **76**, 531 (1949).
[31] Kinsey, Bartholomew, and Walker, Phys. Rev. **78**, 77 (1950).
[32] Kinsey, Bartholomew, and Walker, Phys. Rev. **78**, 481 (1950).
[33] Bartholomew, Kinsey, and Walker, Phys. Rev. **79**, 218 (1950); also private communications.
[34] A. B. Martin, Phys. Rev. **56**, 1062 (1939).
[35] W. L. Davidson, Phys. Rev. **57**, 568 (1940).
[36] A. B. Martin, Phys. Rev. **72**, 378 (1947).
[37] W. D. Whitehead and N. P. Heydenburg, Phys. Rev. **79**, 99 (1950).
[38] W. O. Bateson and E. Pollard, Phys. Rev. **79**, 241 (1950).
[39] Duckworth, Woodcock, and Preston, Phys. Rev. **78**, 479 (1950); H. E. Duckworth and R. S. Preston, Phys. Rev. **79**, 402 (1950); also private communications.
[40] Boyer, Gove, Harvey, Livingston, and Deutsch, to be published.

measured at any angle. The solid angle of the counter was defined by a rectangular slit $\frac{3}{4}$ in. high and 0.4 in. wide, 4 in. from the target. A parallel plate ionization chamber was located at the entrance of the target chamber in order to monitor the deuteron beam, and this reduced the deuteron energy to about 14.0 Mev.

IV. DETERMINATION OF Q-VALUES

A. Experimental Procedure

Deuteron and proton energies cannot be measured precisely by the range technique because of the difficulty in measuring the exact range and the uncertainty in the range energy curve. Thus, the Q-values are measured relative to an accurately known Q-value such as the Q-value of the aluminum ground-state proton peak. The Q-equation for a (d, p) reaction for a deuteron of energy E_d, a proton of energy E_p at an angle θ, and a residual nucleus with a mass number A is approximately

$$Q=(1+1/A)E_p-(1-2/A)E_d-(2/A)(2E_pE_d)^{\frac{1}{2}}\cos\theta.$$

From the Q-equation for two proton groups from targets of mass numbers A_1 and A_2 we have

$$\begin{aligned}Q_1-Q_2=&(E_{p1}-E_{p2})-(E_{d1}-E_{d2})\\&-[2A_1^{-1}(2E_{p1}E_{d1})^{\frac{1}{2}}\cos\theta_1-2A_2^{-1}(2E_{p2}E_{d2})^{\frac{1}{2}}\cos\theta_2]\\&+(E_{p1}+2E_{d1})A_1^{-1}-(E_{p2}+2E_{d2})A_2^{-1};\end{aligned}$$

and, hence, the error would be

$$\begin{aligned}\Delta(Q_1-Q_2)=&\Delta(E_{p1}-E_{p2})-\Delta(E_{d1}-E_{d2})\\&+[(2/A_1)(2E_{p1}E_{d1})^{\frac{1}{2}}\sin\theta_1\Delta\theta_1\\&-(2/A_2)(2E_{p2}E_{d2})^{\frac{1}{2}}\sin\theta_2\Delta\theta_2]+\text{terms of order}\\&(\Delta E_{p1}/A_1,\ \Delta E_{d1}/A_1,\ \Delta E_{p2}/A_2,\ \Delta E_{d2}/A_2).\end{aligned}$$

Thus, it is not necessary to measure accurately the deuteron and proton energies but only the difference in energy between the two proton groups and the difference in deuteron energy at the center of each target, since the targets are of different thicknesses. The Q-values are calculated at the center of the target, since a thick target introduces a rectangular spread centered about the protons produced at the center of the target.

The aluminum ground-state peak was selected as a standard, since the ground-state peak is well separated from lower energy groups, thin foils are readily available, and the Q-values to be measured are expected to be in this region. The Q-value adopted for the ground-state peak was 5.50 Mev. The Q-values obtained from range measurements are as follows: Allan and Clavier:[41] 5.50±0.06; Pollard, Sailor, and Wyly:[42] 5.45±0.05; and Whitehead and Heydenburg:[37] 5.71. Recent measurements with magnetic analysis results[43] in a Q-value of 5.50±0.01 Mev with a low lying excited level at 30 kev.

Tests were made to determine how sensitive the deuteron energy was to the various controls of the cyclotron. By keeping the controls within reasonable limits it is estimated that the deuteron energy can be kept constant to 20 to 30 kev.

Data for the light and medium weight elements were run at some forward angle, usually 30°, and the heavy elements at an angle of 50° to 60°. A careful search was made for high energy proton groups of very weak intensities. In many cases, if there had been a peak the order of 1 percent of the highest energy peak observed, it would have been detected. The high energy section of the spectrum was then taken at several angles up to 90° to check that the peaks shifted correctly with angle corresponding to the mass of the target. In many cases, with targets having several isotopes, one isotope is quite abundant (greater than 60 percent) and the ground-state proton peak can be identified from its intensity. Since a lighter isotope will have a higher energy ground-state peak, it can usually be identified. An angle such as 30° was selected and alternate spectra of the aluminum ground-state peak at 30° and the proton peaks from the target were taken. About 10 to 15 points were taken on the aluminum ground-state peak; each point took about 10 seconds. A spectrum of the protons from the other target took about 5 minutes. Several alternate measurements were taken to average out any fluctuation in the deuteron energy or drift in the gate settings. When the alternate spectra showed a fluctuation in range of more than 1 or 2 mg/cm² of Al (about 30 kev), the data were taken again. These alternate spectra were averaged, and the difference in the ranges of the two peaks was measured; and thus the difference in energy of the two proton groups determined. We must also correct for the proton energy loss in the target.

The procedure for computing the Q-value from the target was as follows. From the mean range of the aluminum ground-state protons (corrected for a half-target thickness) we obtain the proton energy at the center of the target, and then we compute the deuteron energy from the Q-equation. Correcting for the deuteron energy loss in a half-target thickness we obtain the incident deuteron energy. We now compute the deuteron energy and the proton energy at the center of the other target and then calculate the Q-value of the other peak. Because we are dealing with quite high energies, one might expect that it would be necessary to use the relativistic Q-equation. For the aluminum ground peak at 90° the difference amounts to 11 kev, but is only 1 kev at 30°. The difference is negligible for heavy elements. Also we have used the mass number A instead of the exact mass M. For the aluminum ground-state peak at 90° the difference is 13 kev; but at 30° it is only 2 kev. This difference is also negligible for heavy elements.

[41] H. R. Allan and C. A. Clavier, Nature **158**, 832 (1946).
[42] Pollard, Sailor, and Wyly, Phys. Rev. **75**, 725 (1949).
[43] High Voltage Lab., M.I.T., private communication.

B. Analysis of Experimental Uncertainties

Counter Angle θ

Assuming that Q_2 is the accurately known Q-value, then the error in Q_1 due to the uncertainty in the counter angle θ is

$$(\Delta Q_1)_\theta = (2/A_1)(2E_{p1}E_{d1})^{\frac{1}{2}} \sin\theta_1 \Delta\theta_1 - (2/A_2)(2E_{p2}E_{d2})^{\frac{1}{2}} \sin\theta_2 \Delta\theta_2.$$

Thus for a given error in θ, the minimum error in Q for a heavy nucleus is obtained for small angles for a heavy reference nucleus. However, elements heavier than aluminum either do not have well-resolved ground-state peaks or their Q-values are not accurately known. This is the reason for selecting aluminum for a reference and choosing an angle of 30°. The counter can be aligned to the deuteron beam to an accuracy of about 1°. There are two small effects that change the effective angle of the counter. One effect, owing to the finite solid angle and size of the deuteron beam on the target, increases the angle. At 30° the effective counter angle is increased by about 0.5°. The other small effect is a result of the angular distribution of the protons. Since for light elements the distribution is strongly forward, the effective angle is less than the measured angle. However, since the aluminum ground-state peak has a maximum[44] at 30°, this second effect is not present. For the aluminum ground-state peak at 30° with 13.9-Mev deuterons and 19-Mev protons, an error in angle of 1.5° results in an error in the Q-value for a heavy nucleus of 20 kev.

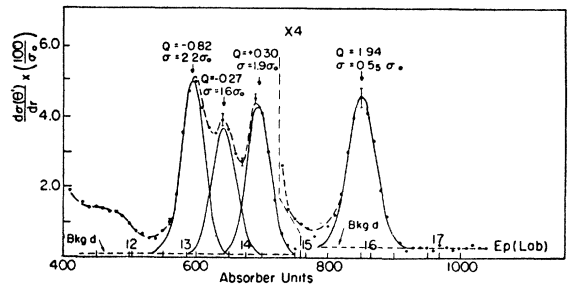

FIG. 1. Proton spectrum at $\theta=50°$ from a 10-mg/cm² bismuth target bombarded with 14-Mev deuterons from the reaction $Bi^{209}(d, p)Bi^{210}$. The ordinate is the differential cross section in the center-of-mass system per absorber unit in terms of the ground-state proton peak from aluminum $(\sigma_0)\cdot\sigma_0=2.5\pm1.0\times10^{-27}$ cm²/steradian. θ' is the angle measured in the center-of-mass system. The abscissa is in units of 0.416 mg/cm² of Al. The proton energy in the laboratory system is also given. The vertical bar represents the square root of the number of counts.

Range of Protons R

The center of the proton peak is chosen as a measure of the mean range of the proton group, since this corresponds to the protons produced at the center of a thick target. The range is measured in absorber units, which are then converted into mg/cm² of aluminum by the conversion factor that 1 absorber unit = 0.416 mg/cm² of aluminum. To the range measured in the foil changer must be added the thickness of foils and gas in the triple counter (10 mg/cm²). There are two other small corrections to be applied to the range. By changing the gate settings, the peak can be made to shift in range. This correction can be approximately determined by comparing a differential and an integral run. For the gate settings used, this correction amounted to about 4 mg/cm². The other small effect is due to the large solid angle and the size of the deuteron beam on the target. Thus, the protons do not pass through the foils exactly at right angles. The average angle is about 4° from the normal, resulting in a correction of 1.5 mg/cm² for the aluminum ground-state peak. The mean range is accurate to a few mg/cm². The difference between the range of 2 proton peaks is accurate to 1 mg/cm² (20 kev).

Range-Energy Curve

The range-energy curve used is that calculated by Smith.[45] Assuming that the computed values for the energy loss per mg/cm² are accurate to 1 percent, the difference in energy of the two proton groups will be accurate to 1 percent.

Energy Loss in Target

In order to obtain sufficient counting rates, targets were of the order of 20 mg/cm² thick. Since the center of the proton peak is taken as a measure of the proton energy, Q-values must be calculated at the center of the target. Bethe and Livingston[46] have calculated the atomic stopping power of various elements at different proton energies. This can be converted into mg/cm² of the various elements equivalent to 1 mg/cm² of aluminum. For a 20-mg/cm² lead target, the deuteron energy loss is about 200 kev in reaching the center of the target and the proton energy loss another 100 kev. Thus, it is necessary that the measured mass/cm² and the calculated conversion values be accurate to 5 percent. Therefore, it was decided to measure the thickness of all targets for 14-Mev deuterons and for high energy protons. This was done by inserting the target in the deuteron beam or the ground-state aluminum protons and measuring the shift of the aluminum ground-state peak at 30°. Since in both cases the target thickness is measured over the same central region as is bombarded, this eliminates errors due to the non-uniformity of the foils. The target thickness for the deuteron beam and for the protons can be measured to 20 kev, and thus the half-target thickness is accurate to 10 kev. The error due to uncertainty in the target angle is negligible.

C. Factors Contributing to the Spread

Since the proton peaks are broad (full width at half-maximum is 500 kev for the aluminum ground-state

[44] H. E. Gove, Phys. Rev. **81**, 364 (1951).

[45] J. H. Smith, Phys. Rev. **71**, 32 (1947).

[46] M. S. Livingston and H. A. Bethe, Revs. Modern Phys. **9**, 272 (1937).

peak), a careful study must be made of the factors which contribute to the spread to justify the choice of the center of the peaks as a measure of the proton energy for all targets. If the observed high energy peak is too broad, then it must be resolved into two peaks, as will be shown in detail later. In order to determine how the width of the proton peak will vary with proton energy and the different targets, one must know the factors which cause the spread and how they vary. For a thin aluminum target, the half-width at $1/e$ of the maximum is 34 absorber units. The factors contributing to this spread are as follows: straggling[47]—23.5, deuteron energy—11, solid angle spread—8, gate settings—14, and other effects—15. The distributions are approximately Gaussian and the numbers are the half-widths in absorber units at $1/e$ of the maximum. When thick targets are used, there is another spread in range introduced, since the (d, p) reaction can occur at any depth of the target. Assuming a constant cross section, the target thickness introduces a rectangular spread centered about the protons produced at the center of the target. This rectangular distribution must be combined with a Gaussian distribution. A 20-mg/cm^2 aluminum target has been run, and the calculated curve fits the observed points very well. The Q-value for the thick target agreed to within 10 kev of the Q-value for a thin target.

D. Differential Cross Sections

Since alternate spectra were taken on the aluminum ground-state peak and the target proton peak, the differential cross section can be evaluated readily in terms of the differential cross section of the aluminum ground-state peak. The relative cross sections are accurate to about 20 percent. The absolute differential cross section (σ_0) of the aluminum ground-state peak at 30° has been measured by Gove[48] and is $2.5\pm1.0 \times10^{-27}$ cm^2/steradian/atom. Counting rates have been converted into a scale of differential cross section/absorber unit/atom of the target.

E. The Ground-State Peaks of $C^{12}(d, p)C^{13}$ and $N^{14}(d, p)N^{15}$

In order to test the method for determining the width of the peaks and for calculating Q-values for thick targets where the Q-values are several Mev different from the aluminum ground-state Q-value, the ground-state peaks of carbon and nitrogen were measured. Thick targets of polyethylene and nylon were run at 30°. The calculated curves fit the observed points very closely. The Q-values calculated from the center of the peaks are 2.70 ± 0.03 and 8.63 ± 0.03 Mev. These agree with the accurately measured Q-values of 2.717 ± 0.004 and 8.615 ± 0.006 Mev.[49]

[47] H. A. Bethe, *The Properties of Atomic Nuclei II*, (Brookhaven National Laboratory, June 1, 1949), unpublished.
[48] H. E. Gove and K. Boyer, Phys. Rev. **79**, 241 (1950).
[49] B. Malm, Doctor's thesis, M.I.T., May, 1950.

V. EXPERIMENTAL RESULTS

The nuclei investigated have been grouped into three regions: nuclei containing approximately 126 neutrons, 50–82 neutrons, and approximately 28 neutrons. Preliminary results have been reported previously.[50]

A. Nuclei Containing Approximately 126 Neutrons

The proton energy spectra from nuclei containing almost the magic number of 126 neutrons and very

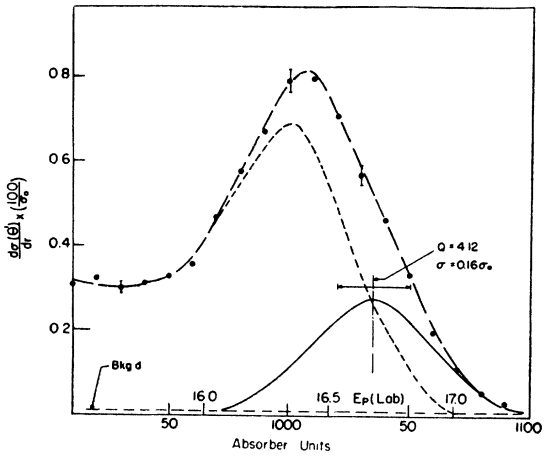

FIG. 2. High energy section of the proton spectrum at $\theta=50°$ from a 20-mg/cm^2 gold target from the reaction $Au^{197}(d, p)Au^{198}$. In this and all succeeding figures of proton spectra the ordinate and the abscissa are the same as for Fig. 1. The lower and upper limits for the position of the ground-state peak are also shown.

nearly the magic number of 82 protons are quite different from spectra of other heavy elements such as gold. The level spacing seems to be quite large in these nuclei near magic number, since the proton spectra from Bi^{209}, Pb^{208}, Pb^{207}, and Pb^{206} targets can be resolved into a few proton groups as shown in Fig. 1. A single peak can be fitted to the long-range proton group from these four targets, as was done for the carbon and nitrogen ground-state peaks. However, in other heavy elements such as tantalum, platinum, gold, thallium, and uranium, the levels are much closer together and the ground-state peak is not well resolved (Fig. 2).

The positions of the ground-state peaks for these cases are determined as follows. One first determines the lower limit for the position of the proton peak by requiring that the calculated curve fit the observed points on the high energy side. When one subtracts this curve from the experimental points, the resultant curve must not drop off more rapidly than the calculated shape. If one fits a curve of shorter range than this lower limit, the calculated curve drops too rapidly on the high-energy side, as shown in Fig. 3.

The upper limit is determined so that the ground-state peak should have a reasonable intensity. The

[50] J. A. Harvey, Phys. Rev. **79**, 241 (1950).

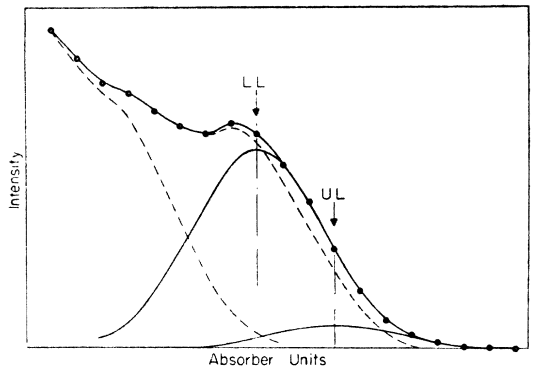

FIG. 3. Procedure for fitting the ground-state proton peak when the ground-state proton group is not well resolved from excited level protons. L.L. represents the lower limit and U.L. the upper limit for the position of the ground-state peak. The dashed curve is the difference between the observed points and the calculated ground-state peak.

criterion adopted was that this upper limit peak contain about 10 percent of the counts in the broad high energy proton peak. By allowing the ground-state peak to have a smaller intensity one can obtain a longer range. Also, the difference between the observed and calculated curves must not fall too steeply.

The results are summarized in Table I. The Q-values for the lead and bismuth targets are the averages for many angles and several targets. Although the other targets have been run at several angles, only one angle was analyzed, since the error in the Q-value depends on this analysis. Table I also contains the differential cross sections for a given angle.

The lead targets were enriched isotopes obtained from the Isotopes Division, Oak Ridge.[51] The Pb^{208} was enriched to 96 percent, the Pb^{207} to 67 percent, and the Pb^{206} to 71 percent. For any target the contributions due to the other two isotopes can be subtracted, since their percentages are known. The thallium target contained 70 percent Tl^{205} and 30 percent Tl^{203}. The observed spectrum has been resolved, so that the ground-state peaks from the two isotopes should have about the same cross section.

B. Nuclei Containing from 50–82 Neutrons

The proton spectra from nuclei with 50 neutrons, such as Sr^{88} and Zr^{90} (Fig. 4), are different from other nuclei in this region such as columbium, molybdenum, rhodium, silver, indium, tin, and antimony (Fig. 5). Again this light nucleus appearance is probably due to the closed shell of 50 neutrons. Table I summarizes the results.

The ground-state peak due to Sr^{88} can be identified, since this is the abundant isotope. A small peak about 2 Mev higher in energy is assigned to Sr^{86}. The ground-state protons due to Sr^{87} would have about 2 Mev higher energy than the Sr^{86} ground-state protons as

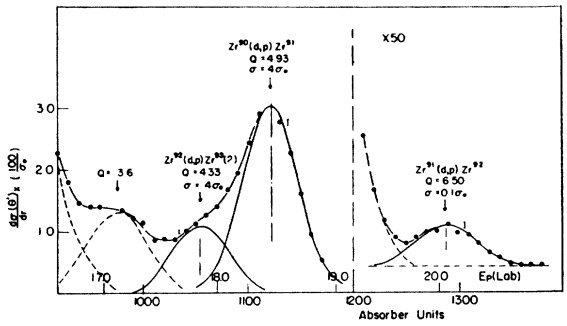

FIG. 4. The high energy section of the proton spectrum at $\theta=20°$ from a 20-mg/cm² zirconium target from the reaction $Zr^{A}(d, p)Zr^{A+1}$.

estimated from the semi-empirical mass formula. This region has been searched and no peak has been found. Thus, we can set an upper limit to its cross section at $0.02\ \sigma_0$.

The ground-state peak of Zr^{90} can be identified readily because of its intensity (Fig. 4). There is also a low intensity peak on the high energy side of the Zr^{90} peak which is assigned to Zr^{91}. If one assumes that

TABLE I. Summary of experimental results for nuclei containing approximately 126 neutrons, 50 and 82 neutrons, and 28 neutrons

Approx. 126 neutrons				Approx. 50 and 82 neutrons				Approx. 28 neutrons			
Target	Angle (θ)	σ/σ_0	Average Q-value	Target	Angle (θ)	σ/σ_0	Average Q-value	Target	Angle (θ)	σ/σ_0	Average Q-value
Bi^{209}	50°	0.55	1.91±0.03	Sr^{88}	30°	1.0	4.32±0.2	Ti^{48}	30°	0.4	5.92±0.05
Pb^{208}	50°	0.6	1.64±0.05	Sr^{86}	30°	0.15	6.29±0.2	Ti^{47}	30°	0.06	8.82±0.4
Pb^{207}	50°	0.10	5.14±0.03	Zr^{90}	20°	4	4.93±0.05	Ti^{46}	30°	0.6	6.51±0.10
Pb^{206}	50°	0.18	4.48±0.03	Zr^{91}	20°	0.1	6.50±0.10	V^{51}	30°	0.6	5.02±0.05
Tl^{205}	30°	0.2	3.93±0.15	$Zr^{92}(?)$	20°	4	4.33±0.10	Fe^{56}	30°	0.8	5.42±0.10
Tl^{203}	30°	0.2	4.29±0.15	Cb^{93}	30°	0.5	5.03±0.10	Fe^{54}	30°	0.5	7.11±0.05
Ta^{181}	30°	0.13	3.80±0.15	Mo^{92}	30°	0.5	6.08±0.2	Co^{59}	15°	0.8	5.43±0.2
Au^{197}	50°	0.16	4.12±0.15	Rh^{103}	30°	0.5	4.58±0.2	Ni^{58}	30°	0.5	6.78±0.10
U^{238}	60°	0.1	2.40±0.15	Ag^{107}	30°	0.5	4.78±0.2	Cu^{63}	15°	0.6	5.55±0.2
Pt^{194}	30°	0.5	3.91±0.2	In^{115}	30°	0.7	4.36±0.2	Zn^{64}	30°	0.7	5.69±0.05
$Pt^{195}(?)$	30°	0.05	5.74±0.2	Sn^{117}	30°	0.3	7.14±0.2				
				Sn^{120}	30°		4.0 ±0.3				
				Sb^{121}	30°	0.6	4.41±0.2				
				Ba^{138}	90°		3.0 ±0.3				

[51] Supplied by Carbide and Carbon Chemical Division, Oak Ridge National Laboratory, Oak Ridge, Tennessee.

the proton spectrum from Zr^{90} is similar to that from Sr^{88}, in that the first excited level to occur will be separated from the ground-state by about 1 Mev, then a peak may be assigned to the ground-state group from Zr^{92}.

The ground-state peaks for other elements in this region were analyzed as explained for gold. Figure 5 shows the proton spectrum from an indium target. Preliminary results have also been obtained from a Sn^{120} target[51] and a barium target.

C. Nuclei Containing Approximately 28 Neutrons

The proton spectra from odd Z isotopes like cobalt and copper indicate a much smaller level spacing than in even Z nuclei like iron, nickel, and zinc. Table I summarizes the results.

The Ti^{48} ground-state peak can be identified by its intensity. A small peak on the high energy side of this peak is assigned to Ti^{46}. Higher energy protons of low intensity result from the odd mass isotopes. The high energy proton spectrum from the Fe^{56} isotope has been resolved into two peaks as shown in Fig. 6. The small high energy peak is assigned to Fe^{54}. The nickel spectrum is very similar to that of iron and gives an excited level in Ni^{59} at 0.4 Mev. Zn^{64} shows a well-resolved ground-state peak. Higher energy peaks from Zn^{67} are not detected.

Figure 7 shows the proton spectrum from a cobalt

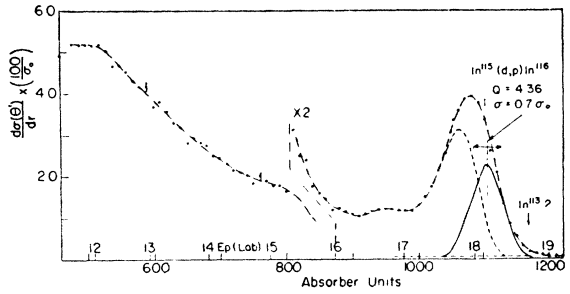

FIG. 5. Proton spectrum at $\theta=30°$ from a 10-mg/cm² indium target from the reaction $In^{115}(d, p)In^{116}$.

target. The ground-state peaks for cobalt and copper were analyzed as explained for gold. The ground-state peak for vanadium was well resolved with the first excited level at 0.8 Mev.

VI. DISCUSSION OF RESULTS

A. Checks for Neutron Binding Energies

Pb^{208}, Pb^{207}, Pt^{195}, *and* Zr^{91}

It was pointed out that the neutron binding energy obtained from the (d, p) method might be only a lower limit. However, if we can also measure the neutron binding energy of the same nucleus from the (γ, n) threshold, or a (d, t) reaction, which set an upper limit, and if the two values agree, then this value must be

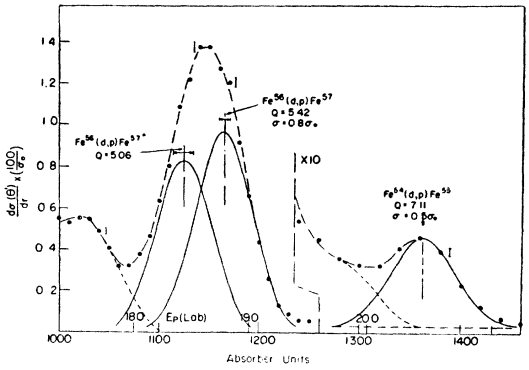

FIG. 6. High energy section of the proton spectrum at $\theta=30°$ from a 20-mg/cm² iron target from the reaction $Fe^{A}(d, p)Fe^{A+1}$.

the correct binding energy. The neutron binding energy of Pb^{208} from the (d, p) and (n, γ) methods is 7.38±0.01 Mev. The value obtained from the (γ, n) threshold is 7.44±0.10 Mev, which agrees. Also the neutron binding energy of Pb^{207} from the (d, p) and (n, γ) method is 6.74±0.01 Mev. The values obtained from the (d, t) and (γ, n) reactions are 6.70±0.05 and 6.93±0.10 Mev, respectively. The (γ, n) measurement is 0.19 Mev too high; but, since the (d, t) value agrees, we can again conclude that this value is correct. The neutron binding energy of Pt^{195} from the (d, p) method is 6.14±0.2 Mev. This agrees with the (γ, n) threshold value of 6.1±0.1 Mev. Finally, the neutron binding energy of Zr^{91} from the (d, p) method is 7.16±0.05 Mev, and from the (γ, n) threshold 7.2±0.4 Mev.

Cu^{64}, Zn^{65}, Fe^{55}, Sn^{121}, *and* Tl^{206}

If we use decay energies[52] or (p, n) thresholds, we can also check several other values. For example, the neutron binding energy for Cu^{64} can be checked as follows. From (γ, n) measurements the neutron binding energy of Zn^{64} is 11.8±0.2 Mev (this may only be an upper limit). From the decay energy of Cu^{64} (0.57 Mev) and the positron energy of Zn^{63} (2.36 Mev) it can be

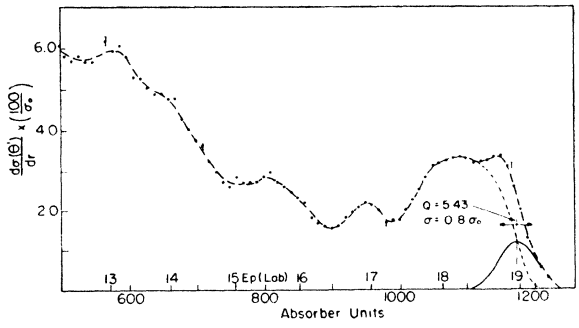

FIG. 7. Proton spectrum at $\theta=15°$ from a 17-mg/cm² cobalt target from the reaction $Co^{59}(d, p)Co^{60}$.

[52] J. Mattauch and A. Flammersfeld, Isotopic Report (1949); G. T. Seaborg and I. Perlman, Revs. Modern Phys. **20**, 585 (1948); D. H. Frisch, M.I.T. Lab. Nuclear Science and Engineering, Technical Report No. 43, table compiled by I. Goldin.

shown readily that the neutron binding energy of Cu^{64} is $\leqq 11.8-(0.57+3.38)=7.85\pm0.2$ Mev. The value obtained from the (d, p) and (n, γ) methods is 7.91 ±0.01 Mev.

Similarly, from the (γ, n) threshold measurement of Cu^{65} (10.2 ± 0.2 Mev), the decay energy of Cu^{64} (0.57 Mev) and the (p, n) threshold of Cu^{65} ($Q=-2.17\pm0.01$ Mev),[53] or the positron energy of Zn^{65} (0.32 Mev), we compute that the neutron binding energy of Zn^{65} is $\leqq 10.2-(0.57+1.39)=8.24\pm0.2$ Mev. This is to be compared with the value of 7.86 ± 0.03 from (d, p) and (n, γ) measurements.

From the (γ, n) threshold of Mn^{55} (10.15 ± 0.2 Mev), the (p, n) threshold[54] of Mn^{55} ($Q=-1.16\pm0.02$ Mev) and the neutron binding energy of Fe^{55} (9.28 ± 0.03 Mev), we can predict the β'-energy of Mn^{54} $E_{\beta'}\leqq 10.15-(9.28+0.38)=0.49\pm0.2$ Mev. It has been reported[55] that there are electrons ~ 1 Mev, but this is not in agreement with the computed value.

From the neutron binding energy of Sb^{121} (9.25 ± 0.2 Mev), the Sn^{121} β-energy (0.38 Mev), and the Sb^{120} positron energy (1.53 Mev), we compute the neutron binding energy of Sn^{121} $\leqq 9.25-(0.38+2.55)=6.32\pm0.2$ Mev. The value obtained from the (d, p) reaction is 6.2 ± 0.3 Mev.

Finally, from the neutron binding energies of Pb^{206} (8.15 ± 0.10 Mev) and Tl^{206} (6.23 Mev), and the β-decay energy of Tl^{206} (1.70 Mev), we can predict the energy difference between Pb^{205} and Tl^{205} (0.22 Mev). Thus, Pb^{205} decays by K-capture.

Pb^{209} *and* Bi^{210}

In order to check the values for Pb^{209} and Bi^{210} we can close the following cycle:

$$\begin{aligned}
&Pb^{206}(d, p)Pb^{207}+Q_1\\
&Pb^{207}(d, p)Pb^{208}+Q_2\\
&Pb^{208}(d, p)Pb^{209}+Q_3\\
&Pb^{209} \xrightarrow{\beta'} Bi^{209}+E_{\beta_1'}\\
&Bi^{209}(d, p)\ Bi^{210}+Q_4\\
&Bi^{210} \xrightarrow{\beta'} Po^{210}+E_{\beta_2'}\\
&Po^{210} \xrightarrow{\alpha} Pb^{206}+He^4+E_\alpha.
\end{aligned}$$

When we add the above relationships, the masses of the heavy nuclei cancel out, and we have left

$$4(M_d-M_p)-M_{He^4}=Q_1+Q_2+Q_3+Q_4+E_{\beta_1'}+E_{\beta_2'}+E_\alpha.$$

The sum of the Q-values and the decay energies is 0.40 ± 0.10 Mev less than the value calculated from the masses. Since the decays of Bi^{210}(RaE) and Po^{210} have been intensively investigated, it is certain that there are no gamma-rays in the disintegrations. Also, it has been reported[52] that there are no gamma-rays in the Pb^{209} β-decay. Preliminary investigations[56] indicate there may be some energy in addition to the β-ray energy. The neutron binding energies predicted by Wapstra[15] agree very well with values derived from Q_1, Q_2, and Q_3. (The maximum difference is 0.19 Mev.) However, Wapstra's computed neutron binding energy of Bi^{210} is 0.55 Mev higher than that derived from Q_4. Since he assumed the decay energy of Pb^{209} to be 0.69 Mev, this indicates that either Q_4 or the Pb^{209} decay energy is not correct. Also, Kinsey, *et al.*,[31] report that the bismuth gamma-ray from neutron capture is broader than expected, and this may be caused by low lying levels in Bi^{210}. There is a level known at 0.047 Mev from the β-decay of Pb^{210}. Thus, it appears that the error is in the Pb^{209} decay. It would be very useful to measure (d, α), (p, α), or (α, p) Q-values in order to check other cycles.

Fe^{55} *and* Mn^{56}

We can also check a few neutron binding energies from mass spectroscopic data. For example, the difference in mass[39] between Fe^{56} and Fe^{54} is 1.99621 amu, from which we calculate that the binding energy of the last two neutrons in Fe^{56} is 20.24 ± 0.3 Mev. Now we can check the neutron binding energies for Fe^{55} and Mn^{56} by the following cycle.

$$\begin{aligned}
&Fe^{54}+n\rightarrow Fe^{55}+9.28\\
&Fe^{55}\rightarrow Mn^{55}+0.38\\
&Mn^{55}+n\rightarrow Mn^{56}+7.25\\
&Mn^{56} \xrightarrow{\beta,\gamma} Fe^{56}+3.63.[57]
\end{aligned}$$

Adding, we get $Fe^{54}+2n\rightarrow Fe^{56}+20.54$ Mev (this may only be a lower limit), which agrees with value calculated from the masses. Thus, this checks all four energies used in this cycle.

Sr^{89} *and* Zr^{90}

Also from masses[39] of Sr^{88} and Zr^{90} we can compute that the mass of Sr^{88} plus two neutrons is greater than the mass of Zr^{90} by 18.5 ± 0.8 Mev. Thus, from the cycle

$$\begin{aligned}
&Sr^{88}+n\rightarrow Sr^{89}+6.55\\
&Sr^{89} \xrightarrow{\beta} Y^{89}+1.46\\
&2.05+Y^{89}\leftarrow Zr^{89}\\
&-12.0+Zr^{89}+n\leftarrow Zr^{90},
\end{aligned}$$

we get

$$Sr^{88}+2n\rightarrow Zr^{90}+18.0 \text{ Mev}.$$

This value checks the value calculated from the masses. However, it does not necessarily prove that the four values used are correct, since two values used allow it to be a lower limit and two values permit it to be an upper limit.

[53] Shoupp, Jennings, and Jones, Phys. Rev. **73**, 421 (1948).
[54] H. T. Smith and R. V. Richards, Phys. Rev. **74**, 1257 (1948).
[55] J. D. Kurbatov and D. Gideon, Phys. Rev. **75**, 328 (1949); Emmerich, Balhueg, and Kurbatov, Phys. Rev. **76**, 1891 (1949).
[56] K. Shure and M. Deutsch, private communication.
[57] K. Siegbahn as reported by Mitchell, Revs. Modern Phys. **22**, 36 (1950).

A few other cycles can be completed but are not of sufficient value to be presented.

B. Computed Neutron Binding Energies

Fe^{56} *and* Ni^{65}

From the neutron binding energy of Mn^{56} (7.25 Mev), the decay energy of Mn^{56} (3.63 Mev), and the mass difference of Fe^{55} and Mn^{55} (0.38 Mev) we can readily compute the neutron binding energy of Fe^{56} as follows:

$$E_n \geqq 7.25+0.38+3.63=11.26 \text{ Mev}.$$

Similarly, the neutron binding energy Ni^{65} is $\leqq 10.2-(2.10+1.68)=6.4$ Mev. In the case of Fe^{56} this might only be a lower limit and in Ni^{65}, only an upper limit.

Rb^{87}, Y^{89}, Sr^{90}, Sr^{91}, Y^{91}, $(Rb^{88}-Sr^{88})$

The neutron binding energies for the above elements have been computed from the neutron binding energies in Sr^{87}, Sr^{89}, Zr^{90} and Zr^{91} and the following total decay energies (in Mev):

Rb^{86}	1.82[58]	Sr^{91}	3.2 ± 0.1[52]
Rb^{87}	0.3 ± 0.1[52]	Y^{88}	~ 3.72[61]
Rb^{88}	5.1[52]	Y^{90}	2.180 ± 0.007[59]
Sr^{89}	1.463 ± 0.005[59]	Y^{91}	1.537 ± 0.007[59]
Sr^{90}	0.54[60]	Zr^{89}	2.05[52].

The computed neutron binding energies are as follows:

$$Rb^{87}=8.5+1.82-0.3=10.0 \text{ Mev}$$
$$Y^{89} \geqq 6.55+1.46+3.72=11.7 \text{ Mev}$$
$$Sr^{90}=7.8+1.46-0.54=8.7 \text{ Mev}$$
$$Y^{90} \leqq 12.0-(2.18+2.05)=7.8 \text{ Mev}$$
$$Sr^{91}=7.8+0.54-3.2=5.1 \text{ Mev}$$
$$Y^{91}=7.16+2.18-1.54=7.8 \text{ Mev}$$
$$Sr^{88}-Rb^{88}=5.1-0.3=4.8 \text{ Mev}.$$

The value for Y^{89} may only be a lower limit and the value for Y^{90} may be an upper limit. The other values may be upper or lower limits, depending on which decay energy is in error.

La^{139}

The neutron binding energy for La^{139} can be computed from the value for Ba^{139}, the decay energy of Ba^{139} (3.5 Mev), and the decay of La^{138}. It has been reported[62] that a 1-Mev γ-ray occurs in the K-capture of La^{138}; thus, this represents a lower limit to the energy. Then the neutron binding energy in $La^{139} \geqq 5.2+(3.5+1.0)=9.7$ Mev.

[58] Zaffarano, Kern, and Mitchell, Phys. Rev. **74**, 682 (1948).
[59] L. M. Langer and H. Clay Price, Phys. Rev. **76**, 640 (1949).
[60] L. J. Laslett, Phys. Rev. **79**, 412 (1950).
[61] W. C. Peacock and J. W. Jones, reported in G. T. Seaborg and I. Perlman, reference 52.
[62] Pringle, Standil, and Roulston, Phys. Rev. **78**, 303 (1950).

TABLE II. Neutron binding energies in the neighborhood of lead.

Z \ $N+1$	122	123	124	125	126	127	128	129	130	131
81	6.54	7.48	6.23	6.97	3.86	5.08	3.00			
82	6.49	8.15	6.74	7.38	3.87	5.20	3.75	5.21		
83				7.44	4.17	5.09	4.41	5.31	3.36	
84			6.71	7.77	4.56	6.01	4.32	5.87	4.08	
85								5.89	4.57	
86									4.7	

Tl, Pb, Bi, Po, At, Em

The neutron binding energies in this region have been predicted by many writers.[10–15] Table II has been computed from the decay energies listed by Wapstra[8] on the assumption that the 0.40-Mev error in closing the lead cycle is due to the Pb^{209} decay. The computed values are not changed if the error is due to the Bi^{210} neutron binding energy. The underlined values are observed values.

C. The Closed Shells of 126, 82, 50, and 28 Neutrons

The neutron binding energy of a nucleus depends on many factors and fluctuates by several Mev, excluding the closed shell effect. For example, nuclei with an even number of neutrons such as Cu^{63} ($E_n=10.9$ Mev) and Cu^{65} ($E_n=10.2$ Mev) have higher neutron binding energies than does a nucleus with an odd number of neutrons such as Cu^{64} ($E_n=7.9$ Mev). This is the θ-term in the semi-empirical mass formula, which gives a value of 3.0 Mev. The semi-empirical mass formula also has a term proportional to $(\frac{1}{2}A-Z)^2$. Thus, the neutron binding energy is greater in the lighter nucleus. For example, the calculated neutron binding energy in Cu^{63} is greater than that in Cu^{65} by 1.0 Mev. Other small effects are caused by the change in the Coulomb energy and the fluctuation in the surface energy. These effects can also be estimated from the semi-empirical mass formula.

From the semi-empirical mass formula,[63]

$$M(A,Z)=A-0.00081Z-0.00611A+0.014A^{\frac{2}{3}}+0.083(\tfrac{1}{2}A-Z)^2A^{-1}+0.000627Z^2A^{-\frac{4}{3}}+\theta,$$

where

$$\delta=0 \text{ for odd } A=\mp\frac{0.036}{A^{\frac{3}{4}}} \text{ } A \text{ even}\begin{cases} Z \text{ even} \\ Z \text{ odd}. \end{cases}$$

We can readily calculate the neutron binding energy for the nucleus $(A+1, Z)$

$$E_n(A+1,Z) \text{ in Mev}=931[M(A,Z)+M_n-M(A+1,Z)]=0.931[15.04+14[A^{\frac{2}{3}}-(A+1)^{\frac{2}{3}}]+83\{(\tfrac{1}{2}A-Z)^2/A-[\tfrac{1}{2}(A+1)-Z]^2/(A+1)\}+0.627Z^2[A^{-\frac{1}{3}}-(A+1)^{-\frac{1}{3}}]+\delta],$$

[63] C. F. v. Weizacker, Z. Physik **96**, 431 (1935); N. Bohr and J. A. Wheeler, Phys. Rev. **56**, 426 (1939); E. Fermi, *Nuclear Physics* (The University of Chicago Press, 1950), p. 7.

TABLE III. Neutron binding energies.

$N+1$ No. of neutrons	$A+1$	Z	(γ, n) thresholds	(n, γ) Kinsey, *et al.*	(d, p) reaction	$(E_n)_{cal}$ B.W.	$(E_n)_{exp} - (E_n)_{cal}$
24	46	22	13.3 ±0.2			12.79	0.4
25	47	22			8.74±0.1	8.24	0.5
26	48	22			11.05±0.4	11.24	−0.2
26	50	24	13.4 ±0.2			12.88	0.5
27	49	22			8.15±0.05	6.91	1.3
28	54	26	13.8 ±0.2			12.96	0.8
29	52	23		7.30	7.25±0.05	6.58	0.7
29	55	26		9.28	9.34±0.05	8.95	0.4
30	55	25	10.15±0.2			10.92	−0.8
30	56	26			≧11.3 (cal.)	11.62	≧−0.3
30	58	28	11.7 ±0.2			13.04	−1.3
31	56	25		7.25	7.2[a]	7.03	0.2
31	57	26		7.63	7.65±0.10	7.76	−0.1
31	59	28		9.01	9.01±0.10	9.23	−0.2
33	60	27		7.73	7.66±0.2	7.43	0.3
34	63	29	10.9 ±0.2			11.31	−0.4
34	64	30	11.8 ±0.2			11.93	−0.1
35	64	29		7.91	7.78±0.2	7.79	0.1
35	65	30		7.86	7.92±0.05	8.43	−0.6
36	65	29	10.2 ±0.2			10.26	−0.1
37	65	28			≦6.4 (cal.)	6.20	≦0.2
40	70	30	9.2 ±0.2			8.97	0.2
42	75	33	10.3 ±0.2			9.78	0.5
44	79	35	10.7 ±0.2			10.00	0.7
46	81	35	10.2 ±0.2			9.22	1.0
48	82	34	9.8 ±0.5			7.99	1.8
49	87	38		8.42	8.52±0.2	7.18	1.3
50	87	37			≈10.0 (cal.)	8.74	≈1.3
50	89	39			≧11.7 (cal.)	9.64	≧2.1
50	90	40	12.0 ±0.2			10.10	1.9
50	92	42	13.28±0.15			11.00	2.3
(50–51)	(88)	(38–37)			≈(4.8 cal.)	(3.2)	≈(1.6)
51	89	38			6.55±0.2	6.53	0.0
51	90	39			≦7.8 (cal.)	7.02	≦0.8
51	91	40	7.2 ±0.4		7.16±0.05	7.46	−0.3
51	93	42			8.31±0.2	8.39	−0.1
52	90	38			≈8.7 (cal.)	8.47	≈0.2
52	91	39			≈7.8 (cal.)	8.94	≈−1.1
52	92	40			8.73±0.10	9.40	−0.7
53	91	38			≈5.1 (cal.)	5.92	≈−0.8
53	93	40			6.56±0.10(?)	6.83	−0.3(?)
53	94	41			7.26±0.10	7.29	0.0
55	97	42	7.1 ±0.3			7.11	0.0
59	104	45			6.81±0.2	7.22	−0.4
60	107	47	>9.5			9.77	>−0.3
61	108	47			7.01±0.2	7.47	−0.5
62	109	47	9.3 ±0.5			9.20	0.1
65	113	48	6.44±0.15			6.80	−0.4
66	115	49	9.5 ±0.5			8.85	0.6
67	116	49			6.59±0.2	6.69	−0.1
68	118	50		9.33	9.37±0.2	8.68	0.7
69	119	50	6.51±0.15			6.57	−0.1
70	121	51	9.25±0.2			8.54	0.7
71	121	50			6.2±0.3	6.12	0.1
71	122	51		7.02	6.64±0.2	6.47	0.2
74	124	50	8.50±0.15			7.30	1.2
74	127	53	9.3 ±0.2 9.45±0.2			8.27	1.1
82	139	57			≧9.7 (cal.)	7.78	≧1.9
82	141	59	9.4 ±0.1 9.8 ±0.3			8.39	1.2
83	139	56			5.2±0.3	5.63	−0.4
90	150	60	7.4 ±0.2			7.16	0.2
108	181	73	7.7 ±0.2			7.49	0.2
109	182	73		6.07	6.03±0.15	5.98	0.1
117	195	78	6.1 ±0.1		6.14±0.2	6.02	0.1
118	196	78			8.0±0.2(?)	7.17	0.8(?)
118	197	79	8.00±0.15 8.10±0.10			7.38	0.6
119	198	79		6.54	6.35±0.15	5.98	0.5
121	201	80	6.25±0.2 6.6 ±0.2			5.94	0.4

TABLE III.—(*Continued*).

$N+1$ No. of neutrons	$A+1$	Z	(γ, n) thresholds	(n, γ) Kinsey, *et al.*	(d, p) reaction	$(E_n)_{cal}$ B.W.	$(E_n)_{exp}-(E_n)_{cal}$
123	204	81		6.54	6.52±0.15	5.89	0.6
124	205	81	7.48±0.15 7.3 ±0.25		7.7±0.2*	7.02	0.5
124	206	82	8.25±0.10		8.10±0.10*	7.21	1.0
125	206	81		6.23	6.16±0.15	5.65	0.6
125	207	82	6.95±0.10 6.9 ±0.1	6.737±0.01	6.71±0.03 6.70±0.05*	5.85	0.9
126	208	82	7.44±0.10	7.38±0.01	7.37±0.03	6.96	0.4
126	209	83	7.45±0.2 7.2 ±0.1		7.44±0.05*	7.16	0.3
127	209	82			3.87±0.05	5.62	−1.75
127	210	83		4.17 ±0.015	4.14±0.03	5.82	−1.65
142	232	90	6.0 ±0.15			6.62	−0.6
143	233	90			4.9±0.2[b]	5.3	−0.4
146	238	92	5.8 ±0.15		5.9±0.2[b]	6.59	−0.7
147	239	92			4.63±0.15	5.34	−0.7

* These values are from the (d, t) reaction.
[a] W. D. Whitehead and N. P. Heydenburg, Phys. Rev. **79**, 99 (1950).
[b] Preliminary result added in proof.

where

$$\delta = \mp \frac{36}{A^{\frac{3}{4}}} \quad A \text{ even} \begin{cases} Z \text{ even} \\ Z \text{ odd} \end{cases}$$

$$= \pm \frac{36}{(A+1)^{\frac{3}{4}}} \quad A \text{ odd} \begin{cases} Z \text{ even} \\ Z \text{ odd.} \end{cases}$$

Table III contains the neutron binding energies determined from (γ, n) threshold measurements,[17,20–26] from the gamma-ray energies in neutron capture,[31–33] and from the (d, p) reaction. Also included in the (d, p) column are a few values from the (d, t) reaction noted by asterisks and the computed values. The calculated values from the semi-empirical mass formula are also listed. The last column is the difference between the observed and the calculated values.

The results are plotted in Fig. 8. Since the (n, γ) measurements are in agreement with the (d, p) measurements, the (n, γ) data have not been plotted. Also, (γ, n) values have not been plotted where (d, t) Q-values were measured. Figure 8 shows sharp discontinuities at 126 and 50 neutrons. The binding energy of the 127th neutron is about 2.2 Mev less than the binding energy of the 126th neutron. Also, the binding energy of the 50th neutron is a little more than 2 Mev greater than the binding energy of the 51st neutron. We can also see that there is another drop in the region of 82 neutrons. In the region of 28 neutrons, there does seem to be a decrease of about 1 Mev. However, this decrease is between 29 and 30 neutrons. If one considers only the (γ, n) data, the decrease is almost 2 Mev. The evidence of the closed shell of 28 neutrons is not very conclusive.

D. The Low Intensity of Ground-State Peaks from Even Z, Odd A Nuclei

The differential cross section of the ground-state peak from an even Z, odd A isotope at forward angles is much smaller than that from an isotope of the same Z but an even A. For the targets where the ground-state peak from an odd isotope was sufficient to be detected (Pt^{195}, Zr^{91}, $Ti^{47,49}$), the differential cross section of the ground-state peak was only about 10 percent that of an even A isotope. Also, for other targets where the intensity was too low to be detected (Sr^{87}, $Mo^{95,97}$, Fe^{57}, and Zn^{67}), we can set an upper limit for their differential cross sections at 10 percent that of an even A isotope. The ground-state peaks from Sn^{117} and Pb^{207}, however, have differential cross sections about one-half

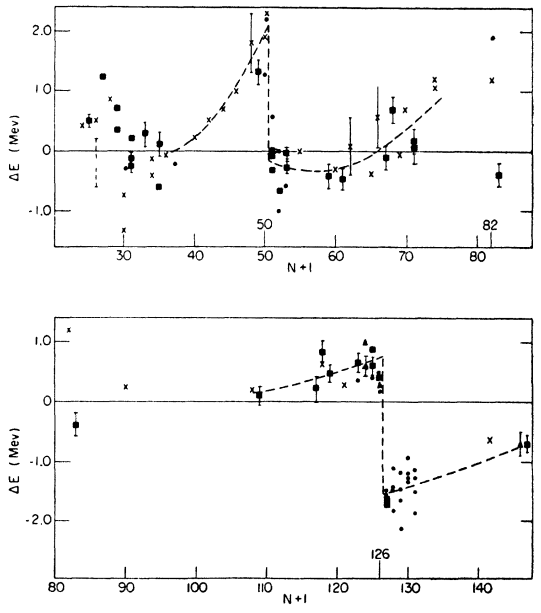

FIG. 8. ΔE is the difference between the observed neutron binding energy for a nucleus with $N+1$ neutrons and the neutron binding energy calculated from the semi-empirical mass formula, plotted *vs* the number of neutrons $N+1$. ■(d, p) reaction with 14-Mev deuterons. ▲(d, t) reaction with 14-Mev deuterons. ×(γ, n) thresholds. ● computed from decay energies.

those of the even Z isotopes. This may be a result of the closed shells of 50 and 82 protons.

The differential cross sections for these even Z, odd A ground-state peaks are low for probably two reasons. First, since the Q-values for these nuclei are larger than for even Z, even A nuclei, their proton energies will be higher. High energy protons are less probable because of the momentum distribution of the proton in the deuteron. The second reason is that the neutron from the deuteron may not pair up with the odd neutron in the target nucleus for nuclear reasons.

The author is indebted to Professors M. Deutsch and M. S. Livingston under whose direction this research was carried out. He would also like to thank M. Deutsch for many helpful criticisms in the preparation of this paper for publication. The equipment was built in collaboration with K. Boyer and H. E. Gove, with whom the author has had many valuable discussions. The cooperation of all the personnel of the Cyclotron Laboratory, Mr. F. J. Fay, Mr. R. W. Kilson, Mr. E. Pulster, and Mr. E. F. White, is gratefully acknowledged. Many of the targets were rolled foils supplied through the kindness of Dr. J. R. Low of the Knolls Atomic Power Laboratory. The chemistry on the separated lead isotopes was done by Mrs. E. Backofen.

APPENDIX

RELATIVE STOPPING POWER OF VARIOUS ELEMENTS

The relative stopping power (relative to aluminum) was measured for 19-Mev protons and 14-Mev deuterons for nearly all of the targets. The values were plotted *vs* Z and a straight line drawn through the points. A few values are compared to values computed from Livingston and Bethe and also to values obtained by Kelly[64] using 28-Mev alpha-particles.

$E_p = 19.0$ Mev

No. of mg/cm² = 1 mg/cm² Al

Element	Experimental	L. and B.	Percent difference
Au	1.82±0.02	1.96	7
Ag	1.42±0.03	1.55	9
Cu	1.20±0.03	1.26	5

$E_d = 14$ Mev

No. of mg/cm² = 1 mg/cm² of Al

Element	Experimental	L. and B.	Percent difference	$E\alpha = 28$ Mev Kelly
Au	2.045±0.01	2.10	2.5	1.99
Ag	1.54 ±0.02	1.61	4.5	1.54
Cu	1.26 ±0.02	1.29	2.5	1.28

[64] E. L. Kelly, Phys. Rev. **75**, 1006 (1949).

PHYSICAL REVIEW VOLUME 81, NUMBER 3 FEBRUARY 1, 1951

Angular Distributions of (d,p) Reactions Using 14-Mev Deuterons*

H. E. GOVE
Laboratory for Nuclear Science and Engineering, Massachusetts Institute of Technology, Cambridge, Massachusetts

(Received September 21, 1950)

The angular distribution of (d,p) reactions for a series of target elements, using 14-Mev deuterons has been investigated. The targets chosen were thin foils of carbon, aluminum, nickel, silver, tantalum, gold, and bismuth. These were bombarded with deuterons from the MIT cyclotron in the center of a large scattering chamber shielded from the cyclotron by 4 ft of concrete. The emitted protons were detected in a triple proportional counter which could be set at any angle from 15° to 135° to the beam. In all cases the measured intensity of protons per unit solid angle is found to be greater in the forward direction. The ratio of the area under the distributions from 20° to 90° to that between 90° and 140° varies from 1.6 to 13. For a given element this ratio increases with proton energy. In addition, for carbon and aluminum, in which individual groups can be resolved, the intensity of protons in a given group, in some cases, exhibits maxima at various angles. In the three elements of highest atomic number the intensity rises from back angles to a maximum at some forward angle and then drops off towards zero degrees. The position of this "turn over" angle appears to increase slowly with atomic number. The general features of the distributions appear to be explainable on a stripping picture rather than that of a compound nucleus.

I. INTRODUCTION

CONSIDERABLE work has been reported on (d,p) angular distributions in the range of deuteron energies from zero to 4 Mev and some work has been done with deuteron energies as high as 7.5 Mev. The purpose of the present work was to study the angular distributions of protons from deuteron-induced reactions at a fixed deuteron energy of 14 Mev over a wide range of atomic number. Detailed studies of (d,p) reactions in the energy range near 15 Mev have been largely neglected and to the best of our knowledge there has been no previous work of this nature reported.

Heydenburg and Inglis[1] have investigated the excitation curves and the angular distributions of proton groups from $O^{16}(d,p)O^{17}$ leaving O^{17} in its ground, and first excited state for deuteron energies between 0.6 and 3 Mev. The excitation curves indicate resonances. The

* Part of thesis submitted in partial fulfillment of the requirements for the degree of Doctor of Philosophy at the Massachusetts Institute of Technology. This work has been assisted by the joint program of the ONR and the AEC. Some of the results have been previously reported at the New York meeting, February, 1950, and the Washington meeting, April, 1950, of the American Physical Society.

[1] N. P. H. Heydenburg and D. R. Inglis, Phys. Rev. **73**, 230 (1948).